Single-Pixel Imaging using Metasurface on Low Light Regime

Randy Stefan Tanuwijaya,* Tsz Kit Yung,† and Jensen T.H. Li‡
Department of Physics
The Hong Kong University of Science and Technology
Clear Water Bay, Hong Kong
(Dated: November 26, 2021)

Optical metasurface has been used to manipulate the photons with minimal loss while maintaining its quantum mechanical properties. We use an optical metasurface sample as a substitute for a parallel beam splitter to induce two-photon interference. Here, we discuss the two advancements made in the current project. First, we developed a method to model a metasurface sample realistically and to analyze and extract parameters (slot dimensions, angle, and separation) of a given metasurface sample Scanning Electron Microscope (SEM) image by using the least-square method. This method is easily extensible to analyze other metasurface patterns as well because this method fits the metasurface image with the lattice equation. Second, we perform simulations for sub-Nyquist single-pixel imaging by using a Hadamard basis. Because the intensity of an image is naturally concentrated at low Hadamard frequency, we can reconstruct the image of an object by using a set of orthogonal filter patterns less than the number of pixels of the object. Finally, we also proposed an experimental setup based on single-pixel coincidence imaging using Spatial Light Modulator (SLM) to generate the filter patterns and a bucket detector to measure the coincidence count.

I. INTRODUCTION

Optical metamaterials have shown several exceptional features those are not possible with natural material, such as negative refractive index [1], superlens [2], and invisibility cloak [3]. Although metamaterial can produce such interesting properties, the thickness has led to extensive loss and causes a lot of challenges in nanofabrication. Due to such limitations, the development of optical metasurface, a thin metamaterial with subwavelength thickness, has emerged in recent years to manipulate the properties of the incident photons with minimal loss. Metasurface has also been shown to be able to manipulate polarization [4] and quantum mechanical properties of light [5].

In our previous report [6], we demonstrated the method and algorithm for coincidence imaging by using a 32x32 pixels TCSPC camera. However, there are limitations of using this method, which is: (1) the image resolution is strictly limited by the resolution of the TCSPC camera; and (2) the camera typically has low photon detection efficiency, mainly when using a weak quantum source, the signal-to-noise ratio is high. To resolve these issues, we propose using the single-pixel imaging method by using SLM and a bucket detector. Single-pixel imaging or ghost imaging has been widely discussed over the past decade, for example, ghost difference imaging [7], Hadamard and Fourier single-pixel imaging [8], super sub-Nyquist single-pixel imaging [9]. The image resolution of the single-pixel imaging method is now limited by the Hadamard filter shown on the SLM, but it is typically higher than the TCSPC camera, around 1280×720 pixels for commercial SLM. Moreover, the bucket photon detector allows for higher photon detector efficiency compared to the TCSPC camera. However, compared to the imaging using the TCSPC camera, this method would require longer image acquisition time as it needs to be exposed to a different layer

Another advancement made in this project is to address the issue encountered in metasurface fabrication, which is the discrepancy between the expected physical properties obtained from the simulation with the actual metasurface sample. Many factors give rise to this discrepancy, one of them being the fabrication imperfections and variations of the dimension and shape of the slot. This work would like to obtain the slots parameter of a given Scanning Electron Microscope (SEM) image by utilizing image processing tools and optimization methods. Moreover, the method used can be easily extended to analyze other metasurface slot patterns.

II. METHODOLOGY

A. Realistic slot model for metasurface characterization

The main idea of constructing such a realistic slot model is adding a finite gradient on the slot edge. One way to accomplish this is by convoluting the step function/the edges of the slot model with a gaussian wave. The resulting function is given by an error function. In the implementation, we convolute a 2D box function with a 2D Gaussian wave to relax the edges. This model accurately portrays the actual slot of the function as the intensity of the FIB laser has a Gaussian distribution. Then we can define a slot cell, a repeating cell in the lattice, by adding multiple slot functions together, with

* rstanuwijaya@connect.ust.hk
† tkyungaa@connect.ust.hk, postgraduate supervisor
‡ jensenli@ust.hk, faculty supervisor

different separation distances and rotation angles. Finally, we can define the slot lattice, which will be used as our fitting function.

This method is essential because the least square method fails to converge when the gradient is not well defined. For example, the slot is naturally modeled using a step function, in which the gradient is 0 everywhere except on edge.

To begin with, we first consider a 1D gasussian distribution $g(x)$ with a standard deviation of σ centered at the origin, and a square function $s(x)$ centered at μ with a width of w.

$$g(x) = \frac{1}{\sqrt{2\pi}\sigma} e^{-x^2/2\sigma^2} \tag{1}$$

$$s(x) = \begin{cases} 1 & \text{for } \mu - \frac{w}{2} < x < \mu + \frac{w}{2} \\ 0 & \text{otherwise} \end{cases} \tag{2}$$

We can convolute these functions to obtain a **flat top gaussian** $f(x)$, which is given by:

$$\begin{aligned} f(x) &= (g * s)(x) \\ &= \frac{1}{2}\left(\text{erf}\left(\frac{\mu + w/2 - x}{\sqrt{2}\sigma}\right) - \text{erf}\left(\frac{\mu - w/2 - x}{\sqrt{2}\sigma}\right)\right) \end{aligned} \tag{3}$$

Then, we can expand this 1D flat top gaussian $f(x)$ into the 2D slot model we needed, which is given by:

$$SlotModel(x, y) = f(x')f(y') \tag{4}$$

Where x' and y' are the transformed coordinate of the slot, for example:

$$\begin{pmatrix} x' \\ y' \end{pmatrix} = \begin{pmatrix} \cos\theta & \sin\theta \\ -\sin\theta & \cos\theta \end{pmatrix} \begin{pmatrix} x \\ y \end{pmatrix} \tag{5}$$

Then for a single slot model, we can use the least-square method to fit the slot model to the given image.

B. Single Pixel Imaging using Hadamard Frequency Analysis

Single Pixel Imaging requires N time-varying lighting or filter patterns S ($m \times n$ pixels) to illuminate the target T ($m \times n$ pixels) and a photon bucket detector to measure the total photon count synchronously. Here S is a binary, either "0" to block the light or "1" to to illuminate the target. The light intensity I_i ($i \in 0...N$) can be calculated by the following equation:

$$I_i = \sum_{x=1}^{m} \sum_{y=1}^{n} S_i(x, y) T_i(x, y) \tag{6}$$

Single Pixel Imaging requires N time-varying lighting or filter patterns S ($m \times n$ pixels) to illuminate the target T ($m \times n$ pixels) and a photon bucket detector to measure the total photon count synchronously. Here S is a binary, either "0" to block the light or "1" to illuminate the target. The light intensity I_i ($i \in 0...N$) can be calculated by the following equation:

The spatial information of the target is the second order intensity correlation function, $G^{(2)}(x, y)$ is given by:

$$G^{(2)}(x, y) = \langle IS \rangle = \frac{1}{N} \sum_{i=1}^{N} I_i S_i(x, y) \propto T(x, y) \tag{7}$$

When $N >> m \times n$ is satisfied, $G^{(2)}(x, y)$ is very close $T(x, y)$. If not, the ghost image will have a high noise level, especially if the filter pattern is random.

After years of development on single-pixel imaging, this method allows for sub-Nyquist conditions and can significantly improve the imaging quality through an orthogonal structured set of filters. One way to construct an orthogonal filter is by using a Hadamard matrix [10], which is a binary matrix composed of "+1" and "-1" and its order is the power of 2. For example, the basis of Hadamard matrix $\mathbf{h}$ is given by:

$$\mathbf{h_2} = \begin{bmatrix} 1 & 1 \\ 1 & -1 \end{bmatrix}; \quad \mathbf{h_{n+1}} = \begin{bmatrix} h_n & h_n \\ h_n & -h_n \end{bmatrix} \otimes \mathbf{h_2} \tag{8}$$

Given a specific Hadamard basis, N mutually orthogonal Hadamard filter can be generated by taking an outer product of any column and row of the Hadamard basis, which is given by:

$$H_i(x, y) = \mathbf{h}(:, u)\mathbf{h}(v, :) \tag{9}$$

However, as a physical filter cannot take a value of "-1", we need to divide the filter pattern H_i into two, namely "H_i^+" and "H_i^-", where $H_i = H_i^+ - H_i^-$ where H_i^+ and H_i^- can only take value of "0" and "1". Therefore, the acquisition of a single intensity value I_i, needs to be done twice with two different filter patterns, and get the difference of the two, as follows:

$$I_i = I_i^+ - I_i^- = \sum_{x,y} H_i(x, y) T(x, y) \tag{10}$$

$$= \sum_{x,y} H_i^+(x, y) T(x, y) - \sum_{x,y} H_i^-(x, y) T(x, y) \tag{11}$$

Then, the image can be reconstructed by calculating the second-order correlation function $G_2(x, y)$ as follows [7]:

$$G^{(2)}(x, y) = \langle IH \rangle = \frac{1}{N} \sum_{i=1}^{N} I_i H_i(x, y) \propto T(x, y) \tag{12}$$

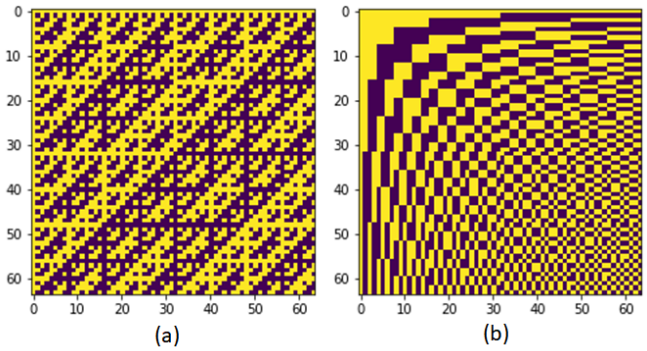

FIG. 1. Hadamard basis matrix for size of 64×64. (a) Natural Hadamard matrix constructed by using the recurrence relation; (b) The hadamard matrix sorted by the number of bit flip in a row/frequency obtained by reordering the natural hadamard matrix.

To achieve the sub-Nyquist condition, i.e., $M < N$, where M is the number of filter patterns, we need to prioritize the filter patterns with the highest intensity. However, it is impossible to determine which filter contributes the most to the image without measuring it. Therefore, we need to use a method to determine the most important filter patterns. One way to do this is by calculating the Hadamard frequency of the image, which is given by the number of bit flip in a row of Hadamard basis, and sorting the rows of the Hadamard basis by the number of bit flip ascending. The reason is in a natural image, there is a **tendency for the pixel with the same brightness to be grouped close with each other**. For this reason, the most important filter patterns H_i are the ones constructed from the lowest Hadamard frequency. Therefore, By sorting the Hadamard basis, we can achieve the sub-Nyquist condition. Figure 1 shows the 64×64 pixels naturally ordered hadamard basis and the frequency-sorted hadamard basis.

III. RESULT

A. Realistic slot model fitting

For our fabrication model, there are some variations of the slot cell used, one of them being two slots per cell separated at a distance d_x, d_y oriented at an angle θ_1 and θ_2. Let the cell dimension being p_x, p_y. Therefore, the slot cell can be defined as:

$$SlotCell(x, y) = SlotModel_1(x, y) + SlotModel_2(x, y) \tag{13}$$

Where $SlotModel_1$ and $SlotModel_2$ are the slots positioned at $\mu_x = p_x \pm d_x/2$ and $\mu_y = p_y \pm d_y/2$ with a rotation angle θ_1 and θ_2 respectively.

The slot lattice is given by repeating slot cells in 2D space. This method can be done by making sure that the slot cell is only defined in the first quadrant, rotating the coordinate with a global rotation angle ϕ, and then taking the modulo of x, y with p_x,p_y. Thus, the analytic lattice function is given by:

$$SlotLattice(x, y) = SlotCell(x \bmod p_x, y \bmod p_y) \tag{14}$$

Finally, we can fit the SEM image with the slot lattice function by using the least-square method. The fitting is done by minimizing the intensity difference between the image and the slot lattice model for all pixels.

To do so, we first preprocess the image by using a **thresholding** method. For example, the thresholding method will set a single pixel intensity to zero if the intensity is below a certain threshold and one otherwise. Then, we can use a **contour extraction** method to select only a pixel patch larger than a specific size to reduce the noise. Finally, we can use a **least-square** method to fit the image with the slot lattice.

Figure 2 illustrates the result of the slot lattice fitting. On the left side, we can see the SEM image of the slot lattice. The lattice is composed of slot cells, which is contains two slots oriented at different angle. The fitting method will be able to determine the parameters of the slot lattice, i.e., the length l and width w of the slot, the slot angles θ_1 and θ_2, the slot separation in x and y axis d_x and d_y, the slot cell dimension p_x and p_y, and the global rotation angle ϕ. The residual plot is shown on the right side, where white illustrates the slot model result and black is the extracted slot after preprocessing the SEM image. We can notice that the some of the slots are missing in the residual plot, which is expected because of the metasurface fabrication error.

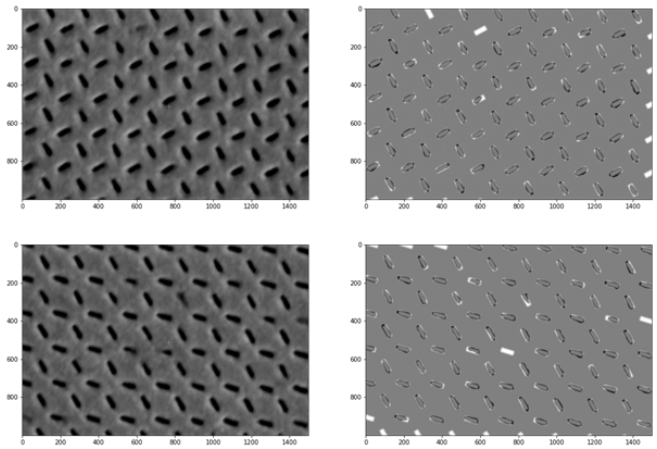

FIG. 2. Result of the metasurface lattice fitting using realistic slot model and least-square method. (left) The SEM image of the metasurface; (right) The residual image after subtracting the slot lattice model from the image, where white is the fitted slot model and black is the extracted slot from the SEM image; (top) the slot pairs oriented at 30° and -60°, and the slot pairs oriented at 30° and 75°.

The slot lattice on the Figure 2, are oriented at $-30°$ - $60°$ (top image) and $30°$ - $75°$. The fitted angle for the first image is $(29.20 \pm 0.02)°$ and $(-60.77 \pm 0.02)°$, and the fitted angle for the second image is $(30.41 \pm 0.02)°$ and $(74.49 \pm 0.02)°$.

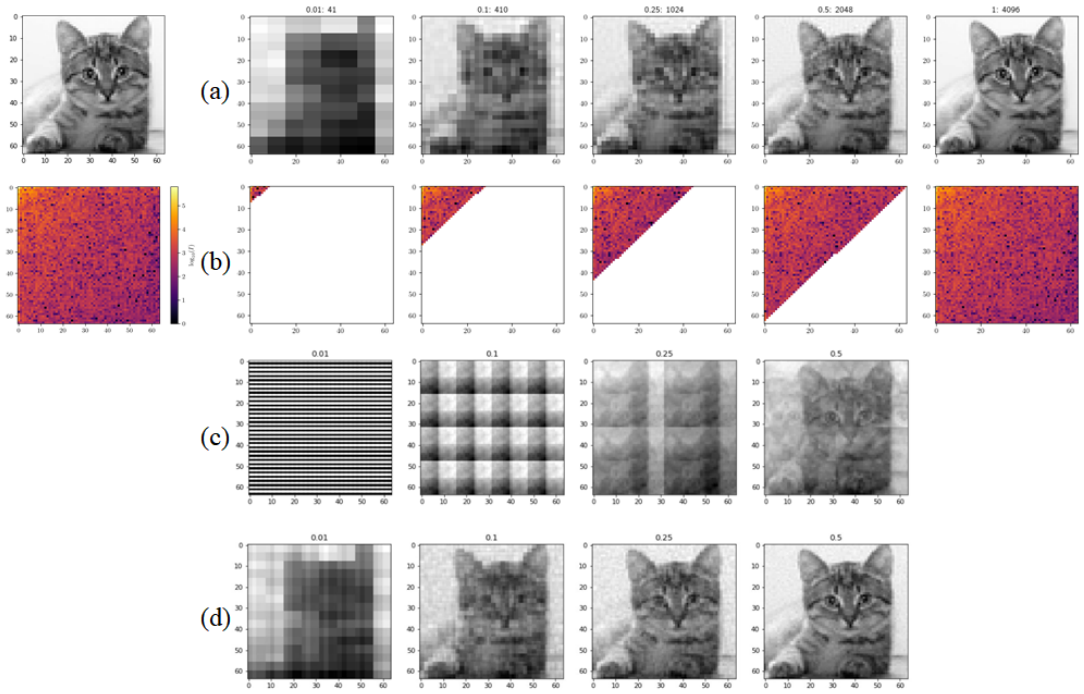

FIG. 3. The simulation result of single-pixel imaging of a cat picture. The leftmost column shows the target image T and the Hadamard frequency spectroscopy of the target image. The columns show the result of single-pixel imaging simulation using the number of filters M equals 1%, 10%, 25%, 50%, and 100% of the number of pixels N. (a) shows the simulation result by using frequency-sorted Hadamard basis; (b) shows the portion of the Hadamard basis used and; (c) shows the simulation result by using the natural order of the Hadamard basis; (d) shows the result of using the intensity ordered filters.

B. Single Pixel Imaging Simulation

We performed a simulation of sub-Nyquist single-pixel imaging using Hadamard frequency analysis. The simulation generates a frequency-sorted Hadamard basis and uses $M < N$ lowest frequency filters to reconstruct the image. The selection of the filter patterns is made by using **zig-zag pathing**. For example, suppose the frequency associated with the Hadamard filter is given by v_x, v_y for the number of bit flip on the row and column in the Hadamard basis, then the associated priority is given by $v_x + v_y$.

Here we use a 64×64 pixels cat picture as a sample target image T. The value of T ranges from 0...255 (dark to bright). We used several M values (1%, 10%, 25%, 50%, and 100% of N) to simulate the sub-Nyquist imaging. Figure 3 shows the result of the single-pixel imaging simulation. The simulation is done by generating a frequency-sorted Hadamard basis and using $M < N$ lowest frequency filters to reconstruct the image by using zig-zag pathing, as shown in the bottom part of the figure 3(a). The peak signal-to-noise ratio (PSNR) of the simulated image is given by: 18.5 (1%), 22.2 (10%), 25.1 (25%), 29.8 (50%).

Figure 3(b) shows the Hadamard frequency spectrum of the image (in log scale). Recall that the frequency is given by the number of bit flip in the Hadamard basis row or column. Notice that the frequency of the image is focused on the low-frequency spectrum, i.e., the top left of the image.

Figure 3(c) shows the simulation result by using the natural order of the Hadamard. Notice that by using the natural order Hadamard, the simulation cannot achieve the sub-Nyquist condition. Figure 3(d) shows the simulation result by using the intensity sorted filter. While this method gives the best resolution possible for a given number of filters M, it is not practical in the experiment as it requires a priori knowledge of the image before mea-

suring the image.

IV. DISCUSSION AND FUTURE WORK

Further to our simulation result, we propose using single pixel imaging method for coincidence imaging. The main advantage of using this method is to obtain higher spatial resolution and to reduce the noise, especailly when using weak quantum source. This is because the photon count produced by the quantum source is very low and SPAD camera photon detection efficiency is not sufficient for measuring the photon intensity. On the other hand, the disadvantage of using single pixel imaging method is that it requires longer acquisition time.

In short, the proposed experimental setup can be described as follows:

1. The source is a quantum source with a frequency of $f_0 \sim 600nm$.
2. The target is an image encoded in the metasurface sample
3. The filter is done by using SLM to generate constructive or destructive interference patterns.
4. The light is propagated through a Barium Bi-Oxide (BBO) crystal, such that it creates an entangled pair of photons on the opposite side of the optical axis.
5. Part of the light is deflected to a detector that functions as a trigger for the bucket detector. If the trigger is activated, the bucket detector will measure the intensity of the light for a certain time.
6. The bucket detector will record the intensity of the light associated with a given filter pattern.
7. The coincidence image can be reconstructed by using the method discussed in the previous section.

V. CONCLUSION

In conclusion, we demonstrated a method to fit and extract the paramaters of a from a metasurface SEM image. This method works by smoothing the edges of a step function by convoluting with a gaussian function and using a least-squares method to fit the image with the slot lattice. This method is easily extensible to extract the parameters of other metasurface patterns as well. Furthermore, we also demonstrated a single pixel imaging simulation by using hadamard basis and frequency analysis. This method can be used for sub-Nyquist single pixel imaging. Finally, we proposed an experimental setup for single pixel coincidence imaging for further work.

[1] R. A. Shelby, Experimental verification of a negative index of refraction, Science **292**, 77 (2001).

[2] J. B. Pendry, Negative refraction makes a perfect lens, Physical Review Letters **85**, 3966 (2000).

[3] D. Schurig, J. J. Mock, B. J. Justice, S. A. Cummer, J. B. Pendry, A. F. Starr, and D. R. Smith, Metamaterial electromagnetic cloak at microwave frequencies, Science **314**, 977 (2006).

[4] A. H. Dorrah, N. A. Rubin, A. Zaidi, M. Tamagnone, and F. Capasso, Metasurface optics for on-demand polarization transformations along the optical path.

[5] A. S. Solntsev, G. S. Agarwal, and Y. S. Kivshar, Metasurfaces for quantum photonics.

[6] R. S. Tanuwijaya, T. K. Yung, and J. Li, Spatial and temporal coincidence measurement on a metasurface in low light regime (2021).

[7] Z. Ye, J. Xiong, and H.-C. Liu, Ghost difference imaging using one single-pixel detector.

[8] Z. Zhang, X. Wang, G. Zheng, and J. Zhong, Hadamard single-pixel imaging versus fourier single-pixel imaging.

[9] X. Yu, R. I. Stantchev, F. Yang, and E. Pickwell-MacPherson, Super sub-nyquist single-pixel imaging by total variation ascending ordering of the hadamard basis.

[10] W. Pratt, J. Kane, and H. Andrews, Hadamard transform image coding.